Certified Control Oriented Learning: A Robust Predictor-Based Approach

Rajiv Singh and Mario Sznaier, *Fellow, IEEE*

***Abstract*—We present a novel approach to the problem of learning the behavior of dynamical systems for the purpose of robust control design. The approach is centered around the derivation of stable predictors of potentially unstable systems and using them to identify plant models that can be ranked by their complexity (order) vs. empirical *Nu*-gap value.**

***Index Terms*—Identification for control, robust control.**

I. Introduction

A GOAL of system identification can be stated as one of deriving a mathematical description of a dynamical system that is no more complicated than what the application demands. The derived model must of course be consistent with both the system measurements as well as any prior knowledge about its behavior and the disturbances. In this context, the goal of *control-oriented* identification is to be able to certify that if the priors are correct, then a controller designed using the identified plant will also stabilize the true, unknown system.

It is well-known that stable, finite-horizon, predictors can be posed even for unstable systems, a fact at the core of the prediction error minimization (PEM) framework [1]. This observation provides the inspiration for the line of approach described in this letter. In short, we lean on the stability of predictors to perform the identification of unstable systems.

In this letter, we discuss approaches to steer the identification process toward *control-friendliness*, that is, trade-off the open-loop closeness of the model's response to the measured one for better closed-loop guarantees. The main tool used for assessing this trade-off is the ν-gap metric that measures the closed-loop distance between systems: specifically, if two systems are close in this metric, then there exists a controller that simultaneously stabilizes both. As discussed in an earlier publication [2], this assessment cannot be done by open-loop measures of the distance between plants.

Approaches that take into account the closed-loop objectives such as the gap metric have been considered under various settings earlier. Some are based on coprime factor identification and typically either require the knowledge of a stabilizing controller beforehand [3], [4], [5], [6], or rely on relaxations that are hard to scale up [7]. Reference [8] minimizes the uncertainty in the identified coprime factors subject to robust stability constraints. However, a prior structure on the transfer function is imposed essentially limiting the role of gap-minimization to a gain K. Reference [2] proposed a generalized interpolation-based approach. In the absence of noise, this method leads to a semi-definite program. However, in the presence of noise, retaining convexity requires using a relaxation that leads to conservative bounds on the uncertainty.

Our objective is to identify a model G_{id} that is as close as possible to the true system G_0 in the gap metric while respecting the uncertainty bounds prescribed on the measurements. Since G_0 is unknown, this can't be achieved directly. Instead, using the prior that the uncertainty bounds envelope the response of G_0, we can estimate the worst-case distance between the true system and the identified model in the gap-metric sense. This is represented by the chord $P_1 - P_2$ in Figure 1 which denotes the distance between the stereographic projections of two response values h_1 and h_2 in the complex plane; see [9] for more details. Assuming h_1 represents the true plant response, the objective then is to find an optimal value for h_2 inside the disk of uncertainty. The standard approach to identifying a stable model that guarantees adherence to the prescribed bounds is using the interpolatory algorithms [10], [11]. Our methodology leverages this approach for control-oriented identification of potentially unstable systems without requiring closed-loop experimentation. Our contributions are as follows:

1) An ersatz scheme for estimating the Chebyshev center of the consistency set in the ν-gap sense.
2) A method for the identification of a robust predictor that can handle both time and frequency domain data.
3) An empirical analysis of the trade-offs between the competing goals of minimizing the ν-gap and keeping the order of the identified model low.
4) Illustration of the efficacy of the proposed approach on a system that is not strongly stabilizable.

Manuscript received 17 March 2023; revised 28 May 2023; accepted 4 June 2023. Date of publication 14 June 2023; date of current version 30 June 2023. This work was supported in part by NSF under Grant CNS–2038493 and Grant CMMI–2208182; in part by the Air Force Office of Scientific Research (AFOSR) under Grant FA9550-19-1-0005; and in part by the Office of Naval Research (ONR) under Grant N00014-21-1-2431. Recommended by Senior Editor P. Tesi. *(Corresponding author: Mario Sznaier.)*

Rajiv Singh is with The MathWorks, Inc., Natick, MA 01760 USA (e-mail: rsingh@mathworks.com).

Mario Sznaier is with the ECE Department, Northeastern University, Boston, MA 02215 USA (e-mail: msznaier@coe.neu.edu).

Digital Object Identifier 10.1109/LCSYS.2023.3286170

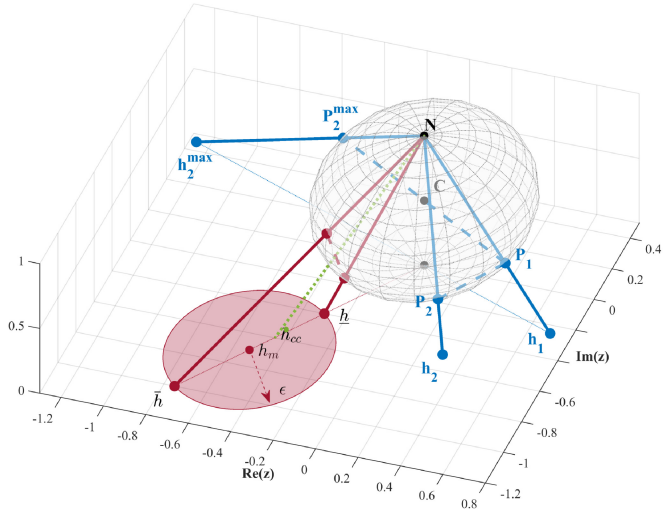

Fig. 1. Stereographic projection and chordal distances. Corresponding to a point $h_1 \in \mathbb{C}$, $\exists\, h_2^{max}$ s.t. the chordal distance between their projections, P_1 and P_2^{max} respectively, is maximized. $\mathbf{N} = (0, 0, 1)$ denotes the "north pole" of the Riemann sphere, and $\mathbf{C} = (0, 0.0.5)$ its center. If $-\bar{h}/|\bar{h}|^2 \notin \mathcal{D}(h_m, \epsilon)$, the Chebyshev center is the point h_{cc} which bisects the projections of the closest ($\underline{h}$) and the farthest ($\bar{h}$) points on the disk (the dotted green line bisects the dashed cherry-colored line and meets the complex plane at h_{cc}).

II. Preliminaries

A. Notation

$G(z) \doteq \sum_{i=0}^{\infty} g_i z^i$ is a discrete-time transfer function that is analytic *inside* the unit disk. $\mathcal{H}_{\infty,\rho}$ denotes space of functions analytic inside the disk of radius $\rho > 1$, equipped with the norm $\|G(z)\|_{\infty,\rho} \doteq \sup_{|z|<\rho} |G(z)|$ (e.g., exponentially stable systems with a stability margin of $\rho - 1$). $\mathcal{H}^{\kappa}_{\infty,\rho}$ denotes the κ-ball in $\mathcal{H}_{\infty,\rho}$, e.g., $\mathcal{H}^{\kappa}_{\infty,\rho} \doteq \{G \in \mathcal{H}_{\infty,\rho}\colon \|G\|_{\infty,\rho} \leq \kappa\}$. We will denote $\mathcal{H}_{\infty,1}$ as simply $\mathcal{H}_{\infty}$. The symbol "$\circledast$" represents the convolution operator. $T_{\mathbf{g}}$ denotes the Toeplitz matrix associated with the impulse response sequence, $\mathbf{g}(t)$, of $G(z)$. $G(z)^{\tilde{}}$ denotes the conjugate of $G(z)$: $G(z)^{\tilde{}} \doteq G^T(1/z)$. Finally, $\nu_{\text{gap}}(G_1, G_2)$ denotes the $\nu-$gap metric between plants G_1 and G_2.

B. Predictor Model

Consider a linear model $\tilde{G}(z)$ that aims to perform the best prediction of the output of another, potentially unstable, linear system $G(z) = B_p(z)/A_p(z)$ one step into the future using all available measurements of $G(z)$ up to a given time instant t. Under a stochastic embedding framework, the optimal predictor can be expressed in terms of the system's true and noise dynamics. For example, consider a Box-Jenkins model structure where the data-generating system contains additive colored noise so that $y_m(t) = B_p(q)/A_p(q)u(t) + C_p(q)/D_p(q)e(t)$, where $y_m(t)$ is the noisy output generated owing to the input $u(t)$ and disturbance $e(t)$, and q denotes the backward shift operator. The optimal predictor (in the prediction mean squared error (MSE) sense) is given by [1]:

$$\tilde{y}(t) = \frac{D_p(q)B_p(q)}{C_p(q)A_p(q)}u(t) + \frac{C_p(q) - D_p(q)}{C_p(q)}y_m(t) \tag{1}$$

The predictor for a single-input single-output (SISO) system is thus another system with one output $\tilde{y}(t)$ and two inputs $u(t)$, and $y_m(t)$. The fundamental assumption underlying the PEM framework is that the predictor is stable. This implies that $C_p(q)$ is a stable polynomial and that the unstable roots of $A_p(q)$ are canceled by those of $D_p(q)$. Succinctly, Eq. (1) can be written as:

$$\tilde{y}(t) = \mathbf{g}_u \circledast u(t) + \mathbf{g}_{y_m} \circledast y_m(t) \tag{2}$$

$$\tilde{Y}(\omega) = H_u(\omega)U(\omega) + H_{y_m}Y_m(\omega) \tag{3}$$

where $\mathbf{g}_u$, and $\mathbf{g}_{y_m}$ denote the impulse responses from $u(t)$ and $y_m(t)$, and $H_u(\omega), H_{y_m}(\omega)$ the corresponding frequency responses. $\tilde{Y}, U, Y_m$ are the Fourier transforms of the corresponding time-domain signals $\tilde{y}$, u, and y_m respectively. In this letter, $\mathbf{g}_u$, $\mathbf{g}_{y_m}$, $H_u(\omega)$, and $H_{y_m}(\omega)$ are the primary design variables. Note that the true plant response can be obtained from that of the predictor as follows:

$$H(\omega) = H_u(\omega)/(1 - H_{y_m}(\omega)). \tag{4}$$

C. Nu-Gap Metric and Robust Stabilizability

Given two SISO models $G_1(z)$, $G_2(z)$ with frequency responses $H_1(e^{j\omega})$ and $H_2(e^{j\omega})$, the ν-gap between G_1, G_2 is given by ([9], Theorem 17.6):

$$\nu_{\text{gap}}(G_1, G_2) = \begin{cases} \|\Psi(H_1(e^{j\omega}), H_2(e^{j\omega}))\|_{\infty} \\ \text{if } \det((I + H_2(e^{j\omega})^{\tilde{}}H_1(e^{j\omega})) \neq 0 \text{ and} \\ \text{wno } \det(I + H_2^{\tilde{}}H_1) + \eta(H_1) - \eta(H_2) \\ -\eta_0(H_2) = 0, \\ 1 \text{ otherwise} \end{cases} \tag{5}$$

where wno denotes the winding number, $\eta(H)$ and $\eta_0(H)$ denote the number of unstable and unit circle poles of G, respectively, and where

$$\Psi(H_1(\omega), H_2(\omega)) \doteq \frac{|H_1(\omega) - H_2(\omega)|}{\sqrt{1+|H_1(\omega)|^2}\sqrt{1+|H_2(\omega)|^2}} \tag{6}$$

The advantage of this expression is that it can be calculated directly from the frequency response data. Given a controller C that stabilizes a certain plant G_1, define:

$$b_{opt} = \left\| \begin{bmatrix} C \\ I \end{bmatrix} (I + G_1 C)^{-1} \begin{bmatrix} I & G_1 \end{bmatrix} \right\|_{\infty}^{-1}$$

Then, if $b_{opt} > \nu_{\text{gap}}(G_1, G_2)$ the controller C also stabilizes G_2 ([9, Th. 17.8]). We will exploit this result to ascertain whether or not a controller designed using the identified model is guaranteed to stabilize the actual plant.

D. Generalized Interpolation Framework for Robust Identification

The generalized interpolation framework, as established in [10], [11] and further used in [12] for finding the minimal order interpolant, generalizes the Nevanlinna-Pick interpolation conditions to incorporate time-domain data. The main result in [10] shows that the problem of finding a function in $\mathcal{H}^{\kappa}_{\infty,\rho}$ that interpolates given time- and frequency-domain measurements can be reduced to a semidefinite program (SDP). For our current purpose, it suffices to recall that a rational interpolant $G(z)$ exists if and only if the following

Hermitian matrix $\mathbf{Z}(H, \mathbf{g}, \rho, \kappa)$ is positive semidefinite:

$$\begin{aligned}
&\mathbf{Z}(H, \mathbf{g}, \rho, \kappa) \doteq \begin{bmatrix} \mathbf{M}_0^{-1} & \frac{1}{\kappa}\mathbf{X} \\ \frac{1}{\kappa}\mathbf{X}^T & \mathbf{M}_0 \end{bmatrix} \succcurlyeq 0 \\
&|H(\omega_i) - H_m(\omega_i)| \leq \epsilon_f, \quad i = 1, 2, \ldots, N_f \\
&|y_m(t) - \mathbf{g}(t) \circledast u(t)| \leq \epsilon_t, \quad t = 1, 2, \ldots, N_t
\end{aligned} \tag{7}$$

where $\mathbf{g}$ denotes the impulse response vector of $G(z)$ and $H(\omega)$ its frequency response. (y_m, u), and $H_m(\omega_i)$ are the corresponding noisy measurements. The matrices $\mathbf{M}_0, \mathbf{X}$ are defined as:

$$\begin{aligned}
&\mathbf{M}_0 = \begin{bmatrix} Q & S_0 R^{-2} \\ R^{-2} S_0^H & R^{-2} \end{bmatrix}, \quad \mathbf{X} = \begin{bmatrix} \mathbf{H} & 0 \\ 0 & T_{\mathbf{g}} \end{bmatrix} \\
&R = diag([1, \rho, \rho^2, \ldots, \rho^{N_t - 1}]) \\
&Q = \left[\frac{\rho^2}{\rho^2 - \bar{z}_i z_j}\right]_{ij}, z_i = e^{j\omega_i T}, \ i, j = 1, 2, \ldots, N_t \\
&S_0 = [\bar{z}_i^j]_{ij}, \ i = 1, 2, \ldots, N_f, \ j = 1, 2, \ldots, N_f \\
&\mathbf{H} = \text{diag}([H(\omega_1), H(\omega_2), \ldots, H(\omega_{N_f})])
\end{aligned} \tag{8}$$

E. Rank Revealing Properties of the Loewner Matrices

Loewner matrices are presented in the context of Lagrange interpolants of rational functions in [13]. Their use for system identification within the generalized interpolation framework is further described in [12]. For the current work, we lean on the rank of an almost square Loewner matrix $\mathbb{L}(H^{N_f}, \boldsymbol{\omega})$ that is composed of frequency response vector H^{N_f} computed over N_f points on the unit circle $z_i = e^{j\omega_i}, \boldsymbol{\omega} \doteq (\omega_1, \ldots, \omega_{N_f})$. If $\text{rank}(\mathbb{L}) = n$, $n < N_f/2$, and all possible n-by-n Loewner submatrices formed using $(H^{N_f}, \boldsymbol{\omega})$ are full-rank, then there exists a unique transfer function corresponding to this data (see [13, Th. 1.2]).

III. Identification of Controls-Friendly Predictors

This section presents the main ideas of this letter.

A. Robust Prediction Using Generalized Interpolation

For robust prediction, we need that prediction errors $e(t) = y_m(t) - \tilde{y}(t)$ are bounded in the worst-case sense, that is, $|e(t)| \leq \epsilon_t(t), \forall t$. This is achieved by using the generalized interpolation formulation.

Lemma 1: Given N_t time-domain samples of input/output data $(u(t), y_m(t))$ and N_f frequency response samples $H_m(e^{j\omega})$, with the following apriori measurement error bounds:

$$|y_m(t) - y(t)| \leq \epsilon_t(t), \forall t = 1, 2, \ldots, N_t \tag{9}$$

$$|H_m(\omega_i) - H(\omega_i)| \leq \epsilon_f(\omega_i), \forall i = 1, 2, \ldots, N_f \tag{10}$$

there exists a set of stable predictors for the plant $G(z)$ provided the following feasibility conditions are met:

$$\begin{aligned}
&Z(H_u, \mathbf{g}_u, \rho, \kappa_1) \succcurlyeq 0 \\
&Z(H_{y_m}, \mathbf{g}_{y_m}, \rho, \kappa_2) \succcurlyeq 0 \\
&|y(t) - \mathbf{g}(t) \circledast u(t)| \leq \epsilon_t(t), \ t = 1, 2, \ldots, N_t \\
&|H(\omega_i) - H_m(\omega_i)| \leq \epsilon_f(\omega_i), \ i = 1, 2, \ldots, N_f
\end{aligned} \tag{11}$$

Proof: See Theorem 3, and proof therein, in [11]. ■

B. Chebyshev Center Approximation

Given measurements $H_m(\omega)$ and the corresponding uncertainty bound ϵ_ω over a grid of ω values, what is the most desirable location of the identified plant response $H_{id}(\omega)$? The ersatz proposed here aims to answer this question.

Let $\mathcal{D}(h_m, \epsilon) \doteq \{ z \in \mathbb{C} \mid |z - h_m|^2 \leq \epsilon^2 \}$ denote the disk of uncertainty of radius ϵ centered at h_m for the measurement at a given frequency. Suppose h_1, h_2 are two feasible points with stereographic projections P_1, P_2 on the Riemann sphere (that is the intersection of the sphere and the lines connecting h_i to the north pole $N \doteq (0, 0, 1)$). The explicit expression for P_i in a coordinate system where the $x - y$ plane is the complex plane is given by:

$$P_i = \left(\frac{Re(h_i)}{1 + |h_i|^2}, \frac{Im(h_i)}{1 + |h_i|^2}, \frac{|h_i|^2)}{1 + |h_i|^2} \right), \ i = 1, 2. \tag{12}$$

Then, $\Psi(h_1(\omega), h_2(\omega))$ defined in (6) is precisely the chordal distance between the projections P_1, P_2. To estimate the Chebyshev center of the uncertainty set $\mathcal{D}(h_m, \epsilon)$, in the gap metric sense, we need to find the points $h_1, h_2 \in \mathcal{D}(h_m, \epsilon)$ such that their corresponding stereographical projections maximize the chordal distance. To this effect, consider a fixed point $h_1 \in \mathcal{D}(h_m, \epsilon)$ and maximize $\Psi(h_1(\omega), h_2(\omega))$ w.r.t. h_2. Tedious algebra shows that the *unconstrained* maximum is achieved for $h_2^{max} = -h_1/|h_1|^2$, with the corresponding $\Psi(h_1(\omega), h_2^{max}(\omega)) = 1$. Geometrically, this corresponds to the case where the chord P_1, P_2^{max} passes through the sphere's center and hence has length 1 (see Figure 1). This observation leads to the following two cases:

B.1. $h_2^{max} \in \mathcal{D}$: This corresponds to the situation where the uncertainty ϵ in a measurement is high relative to its magnitude $|h_m|$. In this case, $\mathcal{D}$ contains the origin, and the chordal distance is maximized by pairs of points contained in the disk such that the chords connecting their projections all pass through the sphere's center. Hence the best guess for the Chebyshev center is $h_{cc} = 0$. This choice supports the commonly known closed-loop objective of small gain at frequencies where the open-loop uncertainty is large.

B.2. $h_2^{max} \notin \mathcal{D}$: This is the more common scenario and is the main focus here. In this case, setting $h_2 = \alpha h_2^{max}$, $0 \leq \alpha < 1$, shows that Ψ is maximized by taking $h_1 = \bar{h}$, the farthest point in $\mathcal{D}$ from the origin, and $h_2 = \underline{h}$, its diametrically opposed point in $\mathcal{D}$. This suggests approximating the Chebyshev center by the point corresponding to the mid-point of the stereographic projections of $\bar{h}$ and $\underline{h}$:

$$h_{cc} = (1 - \gamma)\bar{h} + \gamma \underline{h}, \ \gamma = \frac{1 + |\bar{h}|^2}{2 + |\bar{h}|^2 + |\underline{h}|^2} \tag{13}$$

Remark 1: Note that while h_{cc} is inside the uncertainty disk by construction, it may not belong to the consistency set, since there is no guarantee that there exists a function in $\mathcal{H}_{\infty,\rho}^{\kappa}$ that interpolates these data points. Thus, one may not be able to use h_{cc} directly as the identified plant. Further, when computing h_{cc} we did not impose the winding number condition. Thus h_{cc} is only an approximation (ersatz) to the true center.

C. Main Algorithm

Let $H_{cc}^{N_f}$ denote the N_f-long reference response vector obtained by using the Chebyshev center ersatz (Section III-B). The ersatz indicates that the identification goal should be to stay as close as possible to H_{cc}, at all frequencies, in the gap-metric sense. In the best-case scenario, with no priors other than that the unknown system is linear time-invariant (LTI) and that there are no restrictions on the model order, the identified model response can match H_{cc} arbitrarily well. However, doing so implicitly assumes no additional priors regarding (or preference for) lower-order models, which is often not the case. From an $\mathcal{H}_\infty$-synthesis perspective, it is desirable to keep the plant model order low since the plant order is reflected in the designed compensator order. Thus there is a trade-off between the choice of model order and the achievable gap in the worst case. The following problem statement quantifies this trade-off.

Problem 1: Given noisy time- and frequency-domain measurements, determine the closest stable predictor to H_{cc}, in the ν_{gap} metric, such that the corresponding plant is (a) in the consistency set, (b) has low order, and (c) satisfies (9)-(10).

Proposition 1: Let $\mathbf{g}_{id}^{N_t}$ denote the N_t-long impulse response vector, and $H_{id}^{N_f}$ the N_f-long frequency response vector of the plant to be identified G_{id}. The estimates are obtained as a solution to the following optimization problem:

$$\begin{aligned}
\underset{\Theta}{\textit{Minimize}} \quad & \max_i(\hat{\Psi}_i(H_u, H_{y_m}, \omega_i)) \\
& + \lambda\Big(\text{rank}(\mathbb{L}(H_u)) + \text{rank}(\mathbb{L}(H_{y_m}))\Big) \\
\text{subject to} \quad & Z(H_u, \mathbf{g}_u, \rho, \kappa_1) \succcurlyeq 0 \\
& Z(H_y, \mathbf{g}_y, \rho, \kappa_2) \succcurlyeq 0 \\
& |y(t) - \mathbf{g}(t) \circledast u(t)| \leq \epsilon_t(t) \\
& \frac{|H_m(\omega_i)(1 - H_{y_m}(\omega_i)) - H_u(\omega_i)|}{|1 - H_{y_m}(\omega_i)|} \leq \epsilon_f(\omega_i) \\
& t = 1, \ldots, N_t, \quad i = 1, \ldots, N_f
\end{aligned}$$

where

$$\Theta \doteq \{\mathbf{g}_u, \mathbf{g}_{y_m}, H_u, H_{y_m}, \kappa_1, \kappa_2\} \tag{14}$$

$$\hat{\Psi}_i(\cdot) = \frac{|H_{cc}(\omega_i)(1 - H_{y_m}(\omega_i)) - H_u(\omega_i)|^2}{|H_u(\omega_i)|^2 + |1 - H_{y_m}(\omega_i)|^2} \tag{15}$$

$$\mathbf{g}_u, \mathbf{g}_{y_m} \in \mathbb{R}^{N_t}, \; H_u, H_{y_m} \in \mathbb{C}^{N_f}, \; \kappa_1, \kappa_2 \in \mathbb{R}^+$$

Here (15) uses (4) and (6) to minimize the gap between the identified plant and H_{cc}, while $\lambda \geq 0$ trades off the small ν_{gap} objective against the low order objective for G_{id}. The constraints enforce that G_{id} is in the consistency set.

Proof: Follows from combining (4) and (6)-(8) with the properties of Loewner matrices. ∎

1) Convex Relaxations: We use nuclear norm as a convex relaxation of the matrix rank and further use reweighted trace heuristics to reduce the conservatism introduced by this relaxation [14]. The rational terms in the objective ($\hat{\Psi}_i$) and the frequency domain noise constraint (the last one) can be convexified by using a Sanathanan-Koerner (SK)-type iterative approach wherein a non-convex objective $\min_{a,b} |h - b/a|$ is replaced by the convex objective $\min_{a_k,a_k} |(ha_k - b_k)/a_{k-1}|$ for kth iteration [15]. This leads to the following convex minimization problem (for a single iteration k):

$$\begin{aligned}
\underset{\Theta^{(k)}}{\textit{Minimize}} \quad & J(\Theta^{(k)}) \\
\text{subject to} \quad & Z(H_u^{(k)}, \mathbf{g}_u^{(k)}, \rho, \kappa_1) \succcurlyeq 0 \\
& Z(H_y^{(k)}, \mathbf{g}_y^{(k)}, \rho, \kappa_2) \succcurlyeq 0 \\
& |\tilde{y}(t) - \mathbf{g}_u^{(k)}(t) \circledast u(t) - \mathbf{g}_y^{(k)}(t) \circledast y_m(t)| \leq \tilde{\epsilon}_t(t) \\
& |H_m(\omega_i)(1 - H_{y_m}^{(k)}(\omega_i)) - H_u^{(k)}(\omega_i)|^2 \leq \epsilon_f^2(\omega_i) \mathbb{W}_f^{(k)} \\
& |H_{cc}(\omega_i)(1 - H_{y_m}^{(k)}(\omega_i)) - H_u^{(k)}(\omega_i)|^2 \leq \delta_\nu^{(k)} \mathbb{W}_\nu^{(k)} \\
& t = 1, \ldots, N_t, \quad i = 1, \ldots, N_f
\end{aligned}$$

where

$$\begin{aligned}
J(\Theta^{(k)}) = \delta_\nu^{(k)} + \lambda\Big(& \text{Tr}(\mathcal{W}_{u,1}^{(k-1)} U_1) + \text{Tr}(\mathcal{W}_{u,2}^{(k-1)} U_2) \\
& \text{Tr}(\mathcal{W}_{y,1}^{(k-1)} Y_1) + \text{Tr}(\mathcal{W}_{y,2}^{(k-1)} Y_2)\Big) \\
& + \eta(\Big\| |1 - H_y^{(k)}(\omega)| - \mathbb{W}_f^{(k)} \Big\|_2^2),
\end{aligned} \tag{16}$$

$$\tilde{\epsilon}_t(t) = (1 - \mathbf{g}_y^{(k)}(t)) \circledast \epsilon_t(t); \; U_1, U_2, Y_1, Y_2 \succ 0$$

$$\Theta^{(k)} = \{\delta_\nu^{(k)}, \mathbf{g}_u^{(k)}, \mathbf{g}_y^{(k)}, H_u^{(k)}, H_y^{(k)}, U_1, U_2, Y_1, Y_2, \kappa_1, \kappa_2\}$$

The weights $\mathbb{W}_*^{(k)} \in \mathbb{R}^{N_f}$ are updated in the outer iterative loop. η is the penalty associated with a regularization term that is added to keep the changes over the iterations relatively small. The complete algorithm is summarized in Algorithm 1.

Algorithm 1 Minimization Approach for Problem 1

1: **Inputs:**
   Data: $u(t), y_m(t), H_m(\omega)$ samples
   Priors: $\rho, \epsilon_f(\omega), \epsilon_t(t), \delta_\nu^{min}, \delta_f^{min}$
2: **Initialize:**
   $k = 0$ ▷ iter counter
   Weights: $\mathbb{W}_\nu^{(0)}, \mathbb{W}_f^{(0)}$ (e.g., using PEM)
   $\mathcal{W}_{u,1}^{(0)} = \mathcal{W}_{u,2}^{(0)} = \mathcal{W}_{y,1}^{(0)} = \mathcal{W}_{y,2}^{(0)} = \boldsymbol{I}$
   $\eta = 1e3$, $\epsilon_0 = 1e-4$
3: **while** $\delta_\nu > \delta_\nu^{min}$ | $\delta_f > \delta_f^{min}$ **do**
4: $k \leftarrow k + 1$
5: $\Theta_k \leftarrow argminJ(\Theta^{(k)})$ ▷ Eq. (16)
6: $\mathbb{W}_\nu^{(k)} \leftarrow |H_u^{(k)}|^2 + |1 - H_y^{(k)}|^2$
7: $\mathbb{W}_f^{(k)} \leftarrow |1 - H_y^{(k)}|^2$
8: $\mathcal{W}_{u,*}^{(k)} \leftarrow (U_* + \epsilon_0 \boldsymbol{I})^{-1}$ ▷ $* = 1, 2$
9: $\mathcal{W}_{y,*}^{(k)} \leftarrow (Y_* + \epsilon_0 \boldsymbol{I})^{-1}$
10: **end while**
11: Use Algorithm 1.2 in (13) to find G_{id}

Step 10 of Algorithm 1 yields a candidate identified frequency response H_{id}, The last step obtains a state-space realization, G_{id}, of this response by imposing a cut-off threshold on the singular values of the Loewner matrix $\mathbb{L}(H_{id})$.

2) Other Numerical Aspects: The domain mapping and the linear matrix inequality (LMI) rescaling arguments made in [2] (Section IV-A4) apply here as well. In particular, the feasibility matrices $Z(H_u^{(k)}, \ldots), Z(H_y^{(k)}, \ldots)$ of (11) become ill-conditioned as ρ increases and necessitate the use of both of these techniques.

Remark 2: The output δ_ν of Algorithm 1 is a valid ν_{gap} only if the winding number condition in (5) holds. This can be

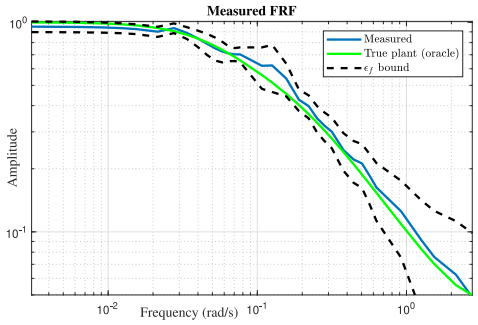

Fig. 2. Measured FRF with uncertainty bounds. The green curve shows the true plant (Oracle) response.

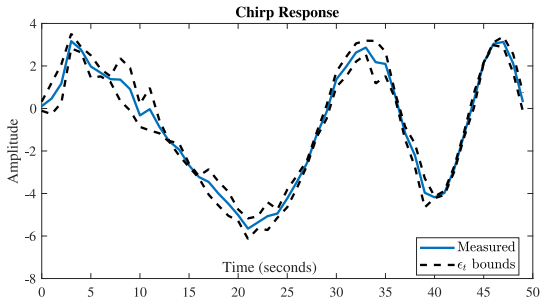

Fig. 3. Measured chirp signal response with prescribed uncertainty bounds.

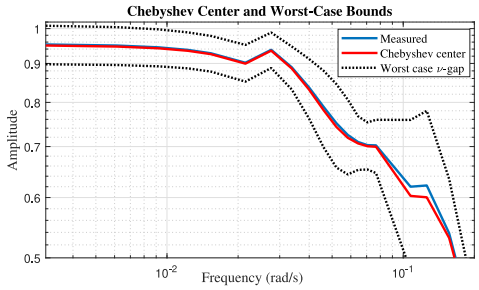

Fig. 4. Estimated Chebyshev center and worst-case ν_{gap} responses. Red: Chebyshev center H_{cc}, Blue: Measured response H_m.

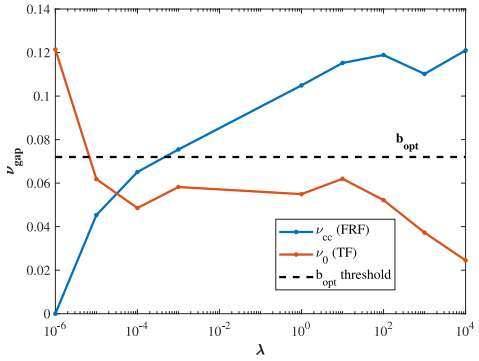

Fig. 5. ν_{gap} vs. λ. ν_{cc} is the chordal distance from the Chebyshev center Hcc. ν_0 is the chordal distance to the true (Oracle) system. "FRF" suffix denotes empirical value computed only on the measurement frequency points (using $\hat{\Psi}$), while "TF" suffix denotes the gap of the identified transfer function.

checked numerically by first estimating the number of unstable poles of H_m from its Bode plot and then plotting $\det(1 + H_{id}\tilde{}H_m)$. In the absence of such knowledge, the most feasible candidate must be determined by trying out all the candidates and picking the one with the largest stability margin (b_{opt}). The chances of finding a plant model with a verifiable ν_{gap} can be improved by generating a set of results corresponding to multiple orders, all corresponding to similar singular values near the cut-off threshold.

IV. Example: Non-Strongly-Stabilizable Plant

Consider the non-strongly stabilizable plant $G(z) = 0.1(z - 1.1)/(z - 0.95)(z - 1.2)$, used previously in [2] to analyze a coprime factor identification approach. The data is collected by simulating the plant in an open-loop setting using band-limited random and chirp profiles. The measured responses are corrupted by additive noise. The random input response is used for deriving an empirical estimate of the frequency response with the Hann window. 33 samples of the frequency response and 50 samples of the chirp signal time-domain response are used for identification. These responses along with their prior uncertainty bounds are shown in Figures 2 and 3. The stability radius prior is taken to be $\rho = 1.01$.

The (per-frequency) worst-case locations of the true and identified plants are at the uncertainty limits, not unexpected for measurements with relatively small uncertainty relative to the response amplitude. The estimated Chebyshev center (Eq. (13)) along with the worst-case limits (in the ν-gap sense) is shown in Figure 4. H_{cc} stays close to measured values H_m.

Assuming that the true plant stays as far as possible from the Chebyshev center at each frequency, the best achievable gap is $\nu_{\text{gap}}(H_{cc}, H_{worst}) \approx 0.121$, where H_{worst} is the response corresponding to the boundary (the dotted black curves in Figure 4). Here the true plant order is assumed to be unknown. If we imposed a prior regarding the order, such as the true order is as small as possible, it is likely to achieve a smaller gap since then the true plant response must be a smoother curve than H_{worst} and closer to H_{cc}.

To investigate the gap versus order trade-off, Algorithm 1 was run with λ values ranging from 0 to $1e4$, leading to the results shown in Figure 5. As expected, as λ is increased, the number of significant singular values of the Loewner matrices, and hence system order, drops, while the ν-gap measured from the empirical H_{cc} ($= \max_i(\hat{\Psi}_i)$) increases (blue line). On the other hand, the gap between the identified and true plants, $\nu_{\text{gap}}(H_0, H_{id})$, decreases (orange line). This is due to the fact that, for larger values of λ, the order of the identified model happens to be closer to the order of the true plant.

The best result, $\nu_{\text{gap}} \approx 0.0245$, is obtained for $\rho = 1.01, \lambda = 1e4$, for the identified model:

$$G_{id}(z) = \frac{0.113(z - 1.105)}{(z - 1.235)(z - 0.949)} \tag{17}$$

The Nyquist plot of $1 + H_0\tilde{}H_{id}$ for this model is shown in Figure 6 which reveals a winding number of zero.

Since G_{id} has 1 unstable pole, the winding number condition is satisfied. Indeed, the estimated value of $\nu_{\text{gap}} \approx 0.0245$ was verified using the `gapmetric` command of MATLAB® Robust Control Toolbox™ [16]. For the true plant, $b_{opt} = 0.072$. This threshold is shown by a dotted black line in

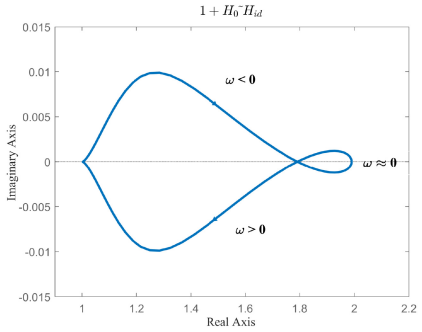

Fig. 6. Nyquist plot of $1 + H_0\tilde{}H_{id}$. There is no encirclement of $z = 0$.

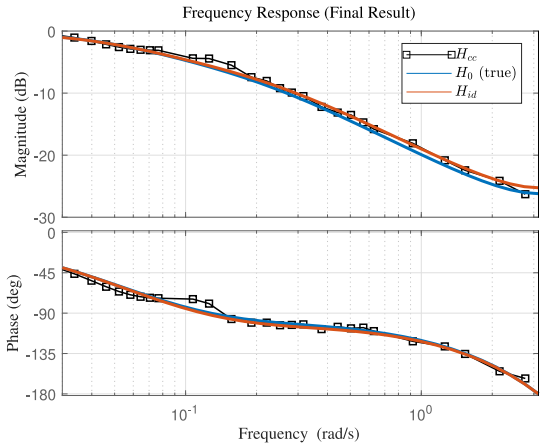

Fig. 7. Frequency response of the best identified model (H_{id}, red) compared against that of the true plant (H_0, blue)) and the empirical Chebyshev center used as fitting data (H_{cc}, red).

Figure 5. Hence it is possible to find identified models with $\nu_{\text{gap}} < b_{opt}$ for many λ values, provided a prior regarding the highest permissible order is placed, which is roughly fourth-order or smaller. Figure 7 compares the identified model's frequency response to the true plant response as well as to the empirical Chebyshev center H_{cc}.

Some final comments regarding the computation time and effectiveness:

- The estimation took 3 iterations of solving (16) using CVX [17] (each iteration $\sim$ 7 minutes, running on a WIN64 PC with 3.6 GHz Intel processor, 64 GB RAM).
- A similar approach but based on coprime factorization was reported earlier [2]. The reported ν_{gap} value was 0.041 for a given choice of the error bounds ϵ_t and ϵ_f. The estimation took roughly half the amount of time as one iteration of Algorithm 1. However, it did not attempt to directly minimize the ν_{gap} or the order of the interpolant model and required ad hoc selection of the error bounds.
- The traditional fit to the data under PEM approach (which does not guarantee worst-case bounds) can be obtained using the `ssest` command of MATLAB® System Identification Toolbox™ [18], under default settings. This yields an 8th order model with 98% fit (in the normalized root means square sense) but producing a gap value of 1.

V. Conclusion

The ultimate goal of control-oriented identification is to generate a model that can be used to synthesize a controller guaranteed to meet given design specifications when combined with the true, unknown plant. This problem is particularly challenging when the unknown plant is open-loop unstable. This letter addresses this scenario from a ν_{gap} perspective. Leveraging the fact that predictors are stable even for unstable plants allows for bringing to bear a generalized interpolation framework to parameterize all candidate models in the consistency set. This parameterization enables searching for models that minimize a composite measure consisting of the ν-gap w.r.t. an empirical Chebyshev center of the feasible model set, and model order, allowing for trading off robustness against model order. These results were illustrated with a non-trivial scenario: identifying a non-strongly stabilizable plant and guaranteeing closed-loop stability of the actual plant using an $\mathcal{H}_\infty$ controller designed with the identified model.

References

[1] L. Ljung, *System Identification—Theory for the User* (Prentice-Hall Information and System Sciences Series), 2nd ed. Upper Saddle River, NJ, USA: Prentice-Hall, 1999.
[2] R. Singh and M. Sznaier, "Certified control-oriented learning: A coprime factorization approach," in *Proc. IEEE 61st Conf. Decis. Control (CDC)*, 2022, pp. 6012–6017.
[3] W. S. Lee, B. D. O. Anderson, R. L. Kosut, and I. M. Y. Mareels, "On adaptive robust control and control-relevant system identification," in *Proc. Amer. Control Conf.*, 1992, pp. 2834–2841.
[4] P. M. J. V. den Hof, R. J. P. Schrama, R. A. de Callafon, and O. H. Bosgra, "Identification of normalised coprime plant factors from closed-loop experimental data," *Eur. J. Control*, vol. 1, no. 1, pp. 62–74, 1995.
[5] T. Zhou, "Frequency response estimation for normalized coprime factors," *Int. J. Control*, vol. 74, no. 4, pp. 315–328, 2001.
[6] T. Oomen and O. Bosgra, "Robust-control-relevant coprime factor identification: A numerically reliable frequency domain approach," in *Proc. Amer. Control Conf.*, 2008, pp. 625–631.
[7] P. Date and G. Vinnicombe, "Algorithms for worst case identification in $\mathcal{H}_\infty$ and in the ν-gap metric," *Automatica*, vol. 40, no. 6, pp. 995–1002, 2004.
[8] C. Q. Zhan and K. Tsakalis, "System identification for robust control," in *Proc. Amer. Control Conf.*, 2007, pp. 846–851.
[9] K. Zhou and J. C. Doyle, *Essentials of Robust Control*. Upper Saddle River, NJ, USA: Prentice-Hall, 1998.
[10] H. Rotstein, "A Nevanlinna-pick approach to time-domain constrained H_∞ control," *SIAM J. Control Optim.*, vol. 34, no. 4, pp. 1329–1341, 1996.
[11] P. A. Parrilo, M. Sznaier, R. S. Sanchez-Pena, and T. Inanc, "Mixed time/frequency-domain based robust identification," *Automatica*, vol. 34, no. 11, pp. 1375–1389, 1998.
[12] R. Singh and M. Sznaier, "A Loewner matrix based convex optimization approach to finding low rank mixed time/frequency domain Interpolants," in *Proc. Amer. Control Conf. (ACC)*, 2020, pp. 5169–5174.
[13] A. C. Ionita, "Lagrange rational interpolation and its applications to approximation of large-scale dynamical system," Ph.D. dissertation, Dept. Comput. Sci., Rice Univ., Houston, TX, USA, 2013.
[14] K. Mohan and M. Fazel, "Reweighted nuclear norm minimization with application to system identification," in *Proc. Amer. Control Conf.*, 2010, pp. 2953–2959.
[15] C. Sanathanan and J. Koerner, "Transfer function synthesis as a ratio of two complex polynomials," *IEEE Trans. Autom. Control*, vol. AC-8, no. 1, pp. 56–58, Jan. 1963.
[16] *MATLAB Robust Control Toolbox Release R2022b*, Mathworks, Natick, MA, USA, 2022.
[17] M. Grant and S. Boyd. "CVX: MATLAB software for disciplined convex programming, version 2.1." Mar. 2014. [Online]. Available: http://cvxr.com/cvx
[18] *MATLAB System Identification Toolbox Release R2022b*, Mathworks, Natick, MA, USA, 2022.